

Hall Effect and Conduction Anisotropy in the Organic Conductor (TMTSF)₂PF₆

G. Mihály,^{1,2} I. Kézsmárki,^{1,2} F. Zámorszky,² and L. Forró¹

¹*IGA, Ecole Polytechnique Federale de Lausanne,
CH-1015 Lausanne, Switzerland*

²*Department of Physics, Technical University of Budapest,
H-1111 Budapest, Hungary
(Received 28 July 1999)*

Both the Hall effect and the ab' -plane conduction anisotropy are directly addressing the unconventional normal phase properties of the Bechgaard salt (TMTSF)₂PF₆. We found that the dramatic reduction of the carrier density deduced from recent optical data is not reflected in an enhanced Hall resistance. The pressure and temperature dependence of the b' -direction resistivity reveal isotropic relaxation time and do not require explanations beyond the Fermi liquid theory. Our results allow a coherent-diffusive transition in the interchain carrier propagation, however the possible crossover to Luttinger liquid behavior is placed at an energy scale above room temperature.

PACS numbers: 74.70.Kn, 71.10.Pm, 71.27.+a

Recent extensive experimental investigations of the low-dimensional organic conductor (TMTSF)₂PF₆ have revealed exciting electronic properties in its metallic phase. The study of the optical conductivity over a wide spectral range led to the puzzling result that the dc conduction along the molecular chains (a direction) is due to only about 1% of the carriers, and the dominant spectral weight is in a high frequency mode above a correlation gap, E_{gap} [1,2]. At low temperatures the system is two dimensional (2D) as evidenced by the observation of a plasma edge along the second most conducting (b') direction [2]. The spin-density wave (SDW) phase transition at $T_{\text{SDW}} = 12$ K is the manifestation of a Fermi-surface anomaly and a broad variety of related phenomena [3,4] is well understood in terms of the imperfect nesting model of a 2D Fermi gas [5]. However, with increasing temperature a 2D \rightarrow 1D dimensionality crossover was suggested, which results in decoupled chains exhibiting Luttinger liquid features [6,7]. The non-Fermi liquid behavior is supported by NMR [8], magnetic susceptibility [9], and photoemission [10] results. The power-low asymptotic dependence of the high frequency optical mode has also been associated to Luttinger exponents [1,7]. The crossover temperature from a low temperature Fermi liquid to a high temperature Luttinger liquid behavior was identified by the resistivity peak measured along the least conducting (c^*) direction [7,11].

The low temperature Fermi liquid state is generally described by a highly anisotropic band structure with transfer integrals in the order of $t_a:t_b:t_c \approx 3000:300:10$ K. The crossover to a non-Fermi liquid state has been related to various possible sources of electronic confinement: (i) to thermal energy exceeding the transverse coupling, $k_B T > t_b$ [6]; (ii) to the decrease of the transverse mean free path below the separation of the chains, $l_b < b$, which leads to the loss of coherence for the interchain transport [12]; and finally (iii) to a correlation gap exceeding the trans-

fer integral perpendicular to the chains, $E_{\text{gap}} > t_b$ [1,13]. It has also been suggested that in these relations a renormalized transfer integral is relevant, t_b^{eff} , which may be substantially smaller than t_b [14]. The nature of the low temperature Fermi liquid phase is also controversial. Here we refer to the reduced number of the carriers participating in dc transport, to the presence of a gapped high frequency mode, and also to the fact that the unusually long relaxation time of $\tau \approx 2 \times 10^{-11}$ s [1] corresponds to an anomalously long mean free path along the chains, $l_a(20 \text{ K}) > 10 \mu\text{m}$.

In order to get insight into the above exotic electrical features of the metallic phase in (TMTSF)₂PF₆ two very basic experiments were carried out for the first time (Hall effect and ab' -plane anisotropy). The number of carriers participating in the electrical transport is deduced from the Hall measurements performed in the temperature range of 5–270 K. The temperature and pressure dependence of the transverse resistivity along the second most conducting direction, ρ_b , was also determined. The results do not reveal evidence for dimensionality crossover up to room temperature and the temperature independent ab' -plane anisotropy suggests isotropic in-plane relaxation time.

The Hall effect was measured in a $B \parallel a$ configuration (magnetic field parallel to the most conducting direction). The current (I) was applied along the c^* direction, while the Hall voltage was measured along the b' direction. Though the experimental realization of such a configuration is hard, it has several advantages. First, in any other configuration the Hall-sensing contacts are placed on well conducting surfaces and thus they are short circuited by the current injecting pads which cover the ends of the crystal. This can be avoided by surface injecting (8-point configuration), but then the current may well be inhomogeneous. Second, as in our case $I \parallel c^*$ the homogeneous current distribution is ensured by the almost equipotential ab' planes. Finally, the application of the magnetic field

does not induce Lorentz force pointing to the c^* direction, along which the development of a Hall field may be influenced by the anions separating the chains.

The results displayed below were obtained on a narrow slice cut from a thick crystal perpendicular to the chain axis. The resulting small piece was $700 \mu\text{m}$ of length (c^* direction), $650 \mu\text{m}$ of width (b direction), and had a thickness $d = 25 \mu\text{m}$ (a direction). The contacts were made by evaporating gold pads on the $b'c^*$ surface of the crystal, and then $6 \mu\text{m}$ gold wires were attached by silver paint. In the six contact arrangements applied, the two pairs of side contacts allowed the simultaneous measurement of the Hall voltage and of the c^* -direction resistance. Measurements on three other crystals gave results consistent with those shown later, however due to their larger thickness they had worse signal/noise ratio.

In order to avoid any systematic error in the Hall voltage (especially the mixing of magnetoresistive components) both the current and the field direction were rotated. The inversion of the magnetic field with respect to the sample was achieved by rotating the crystal by a stepping motor. Most experiments were performed in a persistent mode at $B = 12 \text{ T}$, thus with a fast 180° rotation of the sample we were able to produce a magnetic field change of $\Delta B = 24 \text{ T}$ within 1 s. This was followed by a waiting time of $t_{\text{th}} = 2 \text{ s}$, to let the sample thermalize. Then the Hall resistance, R_H , was measured with inverting currents and applying digital averaging over $t_{\text{av}} = 1 \text{ s}$. This rotation-detection procedure was repeated continuously, and the signal/noise ratio was further improved by taking the average of the data obtained in about 10–50 cycles (over 1–5 min).

The above method was tested in several steps. The thermalization time was chosen long enough to avoid a temperature reading error due to the heating of the sample by the Eddy currents (the good thermalization is shown, for example, by the correct transition temperature determined from the Hall data). Thermal drift or thermal gradient related to the rotations have not influenced the data either. It was tested by changing the order both in the sample rotation sequence and in the current inversion sequence, and the same results were obtained in any of the four combinations. The reproducibility of the data during the cooling and heating cycle was also confirmed. Finally we excluded the possibility of any spurious systematic mechanical error (e.g., the gears applied in the sample holder may have play of about 2°). For this aim we changed the magnetic field of the solenoid from $B = 12$ to -12 T step by step and measured the Hall signal, as described above. This supplied a double check for the inversion of the measured voltage with inverting field. Furthermore, this experiment revealed that the Hall signal is linear up to 12 T, as shown in Fig. 1. (The slight curvature in the Hall voltage can be attributed to the temperature drift that occurred during the more than 1 h measuring time.)

Figures 2 and 3 show the temperature dependence of the Hall resistance of $(\text{TMTSF})_2\text{PF}_6$ in the normal and in

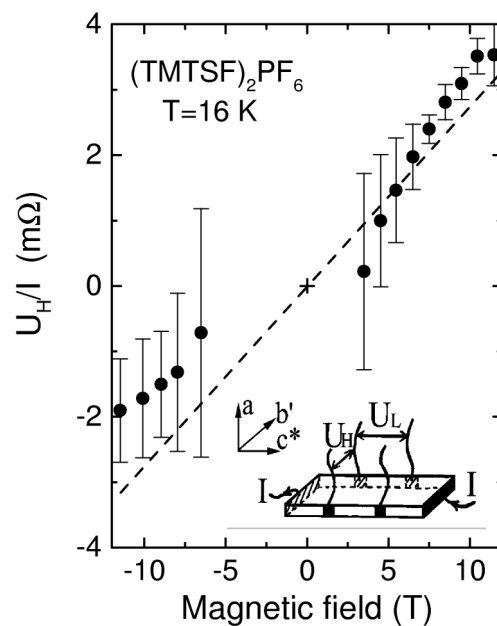


FIG. 1. Magnetic field dependence of the Hall voltage in the metallic phase of $(\text{TMTSF})_2\text{PF}_6$ (for details see text).

the SDW phases, respectively. In the metallic state the Hall signal is small, in accordance with the early observation of Jacobsen *et al.* who determined only an upper limit for it ($|R_H| \lesssim 10^{-2} \text{ cm}^3/\text{C}$ in $B \perp a$ configurations) [15]. We found that the Hall resistance is temperature independent, except in the vicinity of the phase transition. At the transition temperature it changes sign, then in the SDW phase $|R_H|$ rapidly increases 3 orders in magnitude down to $T = 5 \text{ K}$. As expected for a semiconductor, the Hall resistance is activated. The activation energy is $\Delta = 23 \text{ K}$, in accordance with previous results obtained in $B \parallel b'$ configuration [16]. Note, however, that the magnitude of $|R_H|$ measured in the SDW phase when $B \parallel a$ is significantly

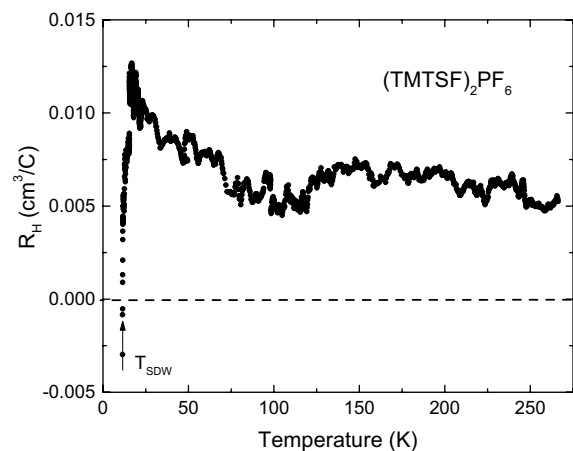


FIG. 2. Temperature dependence of the Hall resistance in the normal phase of $(\text{TMTSF})_2\text{PF}_6$. The carrier density of 1 hole/unit cell corresponds to $R_H = 4 \times 10^{-3} \text{ cm}^3/\text{C}$. The error in the magnitude of the Hall resistance is determined by the accuracy of the thickness measurement ($\pm 30\%$).

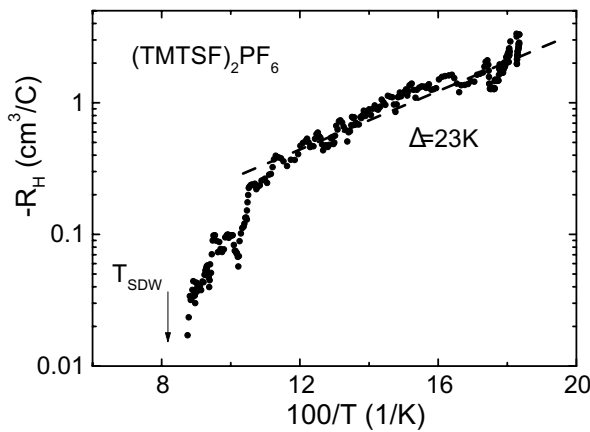


FIG. 3. Arrhenius plot of the Hall resistance in the SDW phase of $(\text{TMTSF})_2\text{PF}_6$.

smaller than that found either for the positive Hall coefficient in the $B \parallel b'$ or for the negative Hall resistance in the $B \parallel c^*$ alignments [16,17].

The resistivity, $\rho(T)$, along the different directions was measured in various four probe arrangements, at samples cut from a thick crystal. In the case of ρ_b four gold strips were evaporated on the $b'c^*$ surface of the crystal, while for ρ_c two pairs of contacts were placed on the opposite ab' surfaces. The typical size of these samples was $0.4 \times 0.4 \times 0.1 \text{ mm}^3$ ($c \times b \times a$). The ab' -plane anisotropy was determined by the Montgomery method [18], as well. In this case the contacts were put on four corners of the ab' side of a long crystal, by placing the gold pads on the opposite ac^* surfaces. We verified that $\rho_a(T)/\rho_b(T)$ calculated from two independent longitudinal measurements agrees with the temperature dependence of the anisotropy determined by the Montgomery method on several crystals, and vice versa, $\rho_a(T)$ or $\rho_b(T)$ calculated from the Montgomery measurements agrees with the results of the direct longitudinal measurements.

Figure 4 shows the temperature dependence of the resistivity measured along the different directions. The a - and c^* -direction data agree well with those published in the literature by various groups. The b' -direction data, however, differ from the single available result published almost 20 years ago [15]. As plotted in Fig. 4, ρ_a and ρ_b exhibit the same temperature profile; the curves scale together. In the normal phase the anisotropy is temperature independent within 20%, its magnitude is $\rho_b/\rho_a = 110 \pm 30\%$. (In small specimens the uncertainty of the contact positions introduces a large scatter in the magnitude of the anisotropy; the above value is the average of six independent measurements.)

The pressure dependence of the resistivity along the a and b' directions was also determined. The samples were inserted into a self-clamping CuBe cell with kerosene as the pressure medium. The results of a Montgomery experiment are shown in Fig. 5 together with the direct a -axis data. The pressure induced variation is the same for both orientations.

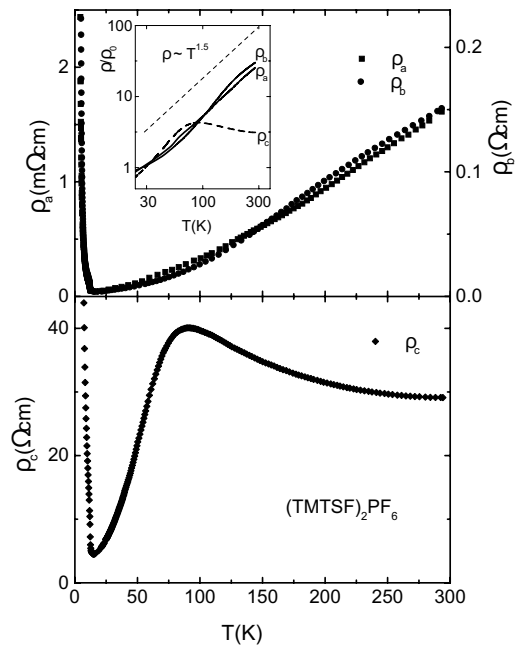


FIG. 4. Temperature dependence of the resistivity measured along the various crystallographic directions. The inset shows the curves on logarithmic scales (normalized at $T = 30 \text{ K}$); the dashed line corresponds to $\rho \propto T^{1.5}$.

In the discussion it will be outlined that all the above observations are consistent with the Fermi-liquid description [19]. Starting with the resistivity data, in contrast to the expectation of the Luttinger liquid picture [7,11], the temperature dependence along the a and b' directions is similar from $T = 30$ to 300 K (Fig. 4). In a good approximation $\rho_a(T) \propto \rho_b(T) \propto T^\alpha$ with $\alpha \approx 1.5$. Though the functional form may change if the isobaric temperature dependence is transformed to constant volume data [11,20] such a transformation modifies ρ_a and ρ_b the same way, since they obey identical pressure dependences (Fig. 5).

The proportionality, $\rho_a(T) \propto \rho_b(T)$, suggests a simple anisotropic band structure with isotropic relaxation time, $\tau(T)$. In a tight binding model a quarter filled band has a conduction anisotropy of $\rho_b/\rho_a = (at_a^2)/(bt_b^2)$. This relation is certainly valid at low temperature where the mean free path along the b direction exceeds the lattice constant:

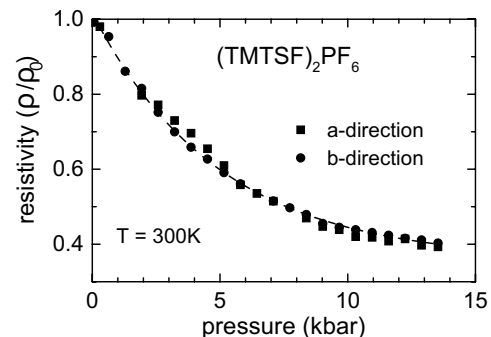


FIG. 5. Pressure dependence of the resistivity measured along the a and the b' directions.

$l_b(20\text{ K}) \approx 20\text{ \AA}$ for $\tau \approx 4 \times 10^{-13}\text{ s}$ [15], $\rho_b/\rho_a \approx 100$ and Fermi velocity, $v_F \approx 4 \times 10^{-7}\text{ cm/s}$ [4]. With increasing temperature $l_b(T)$ decreases below the distance between the chains (7.7 \AA) at $T_X \approx 50\text{ K}$ and above this temperature the interchain carrier propagation becomes diffusive. For such an incoherent interchain motion the perpendicular hopping probability is given by $\tau_b^{-1} = \tau(t_b/\hbar)^2$ [21], i.e., it is determined by the lifetime along the chain direction. As a consequence, even a diffusive b' -direction transport follows the temperature dependence of $\tau(T)$, moreover the magnitude of the anisotropy is the same as in the case of the coherent b' -direction transport (within a factor close to unity) [21].

A coherent-diffusive crossover has not been observed along the c^* direction either, where the mean free path is much smaller [22]. The resistivity anomaly observed in $\rho_c(T)$ (Fig. 4a) can easily be related to the fact that along the c^* direction the chains are separated by the PF_6 anions; thus the transport may rather be characteristic of the hopping process through the anions than of the nature of an ideal anisotropic electron system [22,23]. Note also that around 60 K the proton relaxation data indicate structural rearrangement of the PF_6 ions [24]; thus the conclusions drawn from the c^* -direction transport [7,11] should be taken cautiously.

The Hall effect is a quite general measure of the carrier concentration in metals. The relation $R_H = 1/ne$ is independent of the scattering mechanisms (for isotropic relaxation time, as it is in our case) and remains valid even for a strongly anisotropic band structure [25]. As shown in Fig. 2, the Hall coefficient observed in the normal phase of $(\text{TMTSF})_2\text{PF}_6$ is close to the value $R_H = 4 \times 10^{-3}\text{ cm}^3/\text{C}$ corresponding to a carrier concentration of one hole/unit cell ($n = 1.4 \times 10^{21}\text{ cm}^{-3}$). This is to be contrasted to the proposed factor of 100 reduction of the concentration of the carriers participating in the dc transport [1,2]. Such a reduction should lead to a factor of 100 enhancement in R_H , which obviously has not been observed.

The enhancement of the Hall signal in the vicinity of the phase transition can well be attributed to the opening of a pseudogap due to precursor fluctuations. In the semiconducting phase our results reflect the exponential freezing out of the carriers and the activation energy agrees well with that obtained from the resistivity data. While previous Hall data of $B \parallel b'$ or $B \parallel c^*$ configurations [16,17] led anomalously large Hall mobilities in the SDW phase (explained by introducing in-chain effective mass as small as $1/200m_e$ [16]), our data are consistent with a mean free path of about $\lambda_a(5\text{ K}) \approx 50\text{ \AA}$ for $m \approx m_e$.

In conclusion we performed basic transport experiments in the normal phase of $(\text{TMTSF})_2\text{PF}_6$. The results do not require explanations beyond the Fermi liquid description. The Hall effect corresponds to a carrier density of 1 hole/unit cell and the huge enhancement, expected from the optical data [1,2], was not found. In contrast to previous suggestions based on the c -direction transport

[11] $\rho_b(T)$ does not confirm the Luttinger liquid picture. With increasing temperature a coherent-diffusive transition occurs along the b' direction at $T_X \approx 50\text{ K}$; however this is a smooth crossover and it does not show up in the anisotropy. The incoherent interchain transport still allows strong coupling between chains and for the conduction the conventional Fermi liquid description [21] remains valid. Our results place the possible appearance of the 1D Luttinger liquid features in the dc transport to a higher energy scale (above room temperature): $k_B T > t_b$, the bare transfer integral or $k_B T > E_{\text{gap}}$, the correlation gap observed in optical data.

We thank B. Alavi for sample preparation and G. Gruner, S. Brown, L. Degiorgi, and M. Dressel for useful discussions. This work was supported by the Swiss National Foundation for Scientific Research and by Hungarian Research Funds OTKA T015552 and FKFP 0355-B10.

Note added.—After submission of this article we received a preprint reporting similar Hall results in the normal phase of $(\text{TMTSF})_2\text{PF}_6$ [26].

-
- [1] V. Vescoli *et al.*, *Science* **281**, 1155 (1998).
 - [2] M. Dressel *et al.*, *Phys. Rev. Lett.* **77**, 398 (1996).
 - [3] D. Jerome, in *Organic Conductors*, edited by J. Farges (Marcel Dekker, New York, 1994), p. 405; W. Kang, S. T. Hannahs, and P. M. Chaikin, *Phys. Rev. Lett.* **69**, 2827 (1992); N. Biskup *et al.*, *Phys. Rev. B* **51**, 17972 (1995).
 - [4] F. Zamborszky *et al.*, *Phys. Rev. B* **60**, 4414 (1999).
 - [5] K. Yamaji, *J. Phys. Soc. Jpn.* **51**, 2787 (1982); G. Montambaux, *Phys. Rev. B* **38**, 4788 (1988); G. Mihaly *et al.*, *Phys. Rev. B* **55**, 13456 (1997).
 - [6] C. Bourbonnais *et al.*, *Phys. Rev. Lett.* **62**, 1532 (1989).
 - [7] C. Bourbonnais and D. Jerome, *Science* **281**, 1181 (1998).
 - [8] P. Wzietek *et al.*, *J. Phys. I (France)* **3**, 171 (1993).
 - [9] M. Dumm, A. Loidl, and M. Dressel, *Phys. Rev. B* **61**, 511 (2000).
 - [10] B. Dardel *et al.*, *Europhys. Lett.* **24**, 687 (1993).
 - [11] J. Moser *et al.*, *Eur. Phys. J. B* **1**, 39 (1998).
 - [12] D. G. Clarke *et al.*, *Science* **279**, 2071 (1998).
 - [13] Y. Suzumura *et al.*, *Phys. Rev. B* **57**, 15040 (1998).
 - [14] T. Giamarchi, *Physica (Amsterdam)* **230B–232B**, 975 (1997).
 - [15] C. S. Jacobsen *et al.*, *Solid State Commun.* **38**, 423 (1981).
 - [16] P. M. Chaikin *et al.*, *Phys. Rev. B* **24**, 7155 (1981).
 - [17] L. Forro, *Mol. Cryst. Liq. Cryst.* **85**, 315 (1982).
 - [18] H. C. Montgomery, *J. Appl. Phys.* **42**, 2971 (1971).
 - [19] Recent investigations debate the magnetic field induced crossover to a Luttinger phase, as well. See I. J. Lee and M. J. Naughton, *Phys. Rev. B* **58**, 13343 (1998); G. Kriza *et al.*, *Phys. Rev. B* **60**, 8434 (1999).
 - [20] J. R. Cooper, *Phys. Rev. B* **19**, 2404 (1979).
 - [21] M. Weger, *J. Phys. (Paris), Colloq.* **39**, C6-1456 (1978).
 - [22] J. R. Cooper *et al.*, *Phys. Rev. B* **33**, 6810 (1986).
 - [23] F. Zamborszky *et al.* (to be published).
 - [24] J. C. Scott *et al.*, *Mol. Cryst. Liq. Cryst.* **79**, 41 (1982).
 - [25] J. R. Cooper *et al.*, *J. Phys. (Paris)* **38**, 1097 (1977).
 - [26] J. Moser *et al.*, following Letter, *Phys. Rev. Lett.* **84**, 2674 (2000).